



HAL
open science

Development of a small Time-Projection-Chamber for the quasi-absolute neutron flux measurement

Carole Chatel, Ludovic Mathieu, Mourad Aïche, Maria Diakaki, Olivier Bouland

► **To cite this version:**

Carole Chatel, Ludovic Mathieu, Mourad Aïche, Maria Diakaki, Olivier Bouland. Development of a small Time-Projection-Chamber for the quasi-absolute neutron flux measurement. EPJ Web of Conferences, 2023, 284, pp.01012. 10.1051/epjconf/202328401012 . hal-04309742

HAL Id: hal-04309742

<https://hal.science/hal-04309742v1>

Submitted on 27 Nov 2023

HAL is a multi-disciplinary open access archive for the deposit and dissemination of scientific research documents, whether they are published or not. The documents may come from teaching and research institutions in France or abroad, or from public or private research centers.

L'archive ouverte pluridisciplinaire **HAL**, est destinée au dépôt et à la diffusion de documents scientifiques de niveau recherche, publiés ou non, émanant des établissements d'enseignement et de recherche français ou étrangers, des laboratoires publics ou privés.



Distributed under a Creative Commons Attribution 4.0 International License

Development of a small Time-Projection-Chamber for the quasi-absolute neutron flux measurement

Carole Chatel^{1,2,4*}, Ludovic Mathieu², Mourad Aïche², Maria Diakaki³, and Olivier Bouland⁴

¹Institut Pluridisciplinaire Huber Curien, 23 rue du Loess, 67200 Strasbourg, France

²Laboratoire de Physique des 2 infinis, 33170 Gradignan, France

³National Technical University of Athens, Department of Physics, Zografou Campus, Athens, Greece

⁴CEA, DES/IRENE/DER/SPRC/LEPh, 13008 Saint Paul Lez Durance, France

Abstract. Accurate actinides fission cross sections around 1 MeV are of primary importance for the safety of generation IV reactors. To have accurate measurements, the neutron flux must also be accurately estimated. This is usually done with respect to the $^{235}\text{U}(n,f)$ cross section. It is however possible to measure the neutron flux with respect to the $^1\text{H}(n,n)p$ cross section which is a primary standard, providing an independent and precise measurement. Typically, the usual proton recoil technique uses a silicon detector for neutrons of energy between 1 and 70 MeV. However, the high electron and gamma background due to neutron production under irradiation makes the use of this or any other detector not suitable for an accurate measurement below 1 MeV. To this end, the Gaseous Proton Recoil Telescope is developed and characterized. The goal is to provide quasi-absolute neutron flux measurements with an accuracy better than 3%. It consists of a double ionization chamber with a Micromegas segmented detection plane and the gaseous pressure can be adjusted to protons – and hence neutron – energy. The sensitivity to gamma and electrons background, the intrinsic efficiency as well as the resolution of this detector have been investigated.

1 Introduction

Discrepancies between different measurements around 1 MeV still exist for most of actinides fission cross sections, despite a general great effort from the nuclear community. The neutron fluxes being high in pressurized water reactors (generation II and III) and in fast neutron reactors (generation IV) from few hundreds keV to few MeV, it is of prior importance to reduce the uncertainties in this neutron energy range.

In most of the measurements, fission cross sections are measured with respect to secondary standards ($^{235}\text{U}(n,f)$, $^{238}\text{U}(n,f)$, $^{237}\text{Np}(n,f)$). Their accuracy ranges from 1.3% to 10% between 200 keV and 20 MeV [1]. Moreover, in the energy range we are interested in, the usual reference is mostly $^{235}\text{U}(n,f)$. Thus, the constant use of the same standard creates a strong correlation between different measurements.

For this reason, it has become important to realize an independent and precise measurement using a different neutron flux measurement technique. The use of a primary standard instead of a secondary one, is thus suitable. The $^1\text{H}(n,n)p$ elastic scattering cross section is known with an accuracy ranging between 0.2% to 0.5% from 0 to 20 MeV [1] and reproducible with *ab initio* calculations. This cross section is also structureless, creating no dependence between the measured structures and ones from the reference reaction used.

For a neutron energy range between 1 and 70 MeV, silicon junctions are perfectly adapted as proton recoil detectors [2-5]. However, the desired measurements start around 200 keV (down to the fertile fission thresholds) and Si junction are here no more suitable. Indeed, they are sensitive to a high electron and gamma background under irradiation. As our setup is as close as possible to the neutron source to maximize the flux, many gamma and electrons produced by the source are detected in the recoil-proton detector [2] and adapting the detector thickness is not a sufficient solution [3].

Even if other proton recoil detectors have been developed as plastic scintillator [6-10] or proportional counters [11-13], the inaccuracy of their efficiency makes these detectors not suitable for our goal (see [2, 14, 15] for details).

As no detector seems to already exist to meet all our needs, the ACEN team of the LP2I decided to develop the Gaseous Proton Recoil Telescope (GPRT). This detector should not be sensitive to high electrons/gamma background and able to accurately measure neutron fluxes for neutron energies between 0.2 MeV and 2.5 MeV.

2 GPRT description

The developed detector is a double ionization chamber ($\Delta E-E$). The electric field is generated by the presence

* Corresponding author: carole.chatel@iphc.cnrs.fr

of two electrodes separated by 4 cm of gas. The amplification region is based on a Micromegas technology. It consists of the anode plane (12x4 cm²), segmented in 64 pads and an electrified mesh of the same dimensions, 125 μm above the segmented plane. A field cage is used to homogenize the electric field between the cathode and the mesh [16].

At the entrance of the detector stands a macor sample disk. Its use is to carry several H-rich foils upstream the detector. Then, a first collimator stands as the detector entrance, delimiting part of the detector geometry. A second collimator 2 cm farther delimitates the ΔE chamber from the E one. A picture of the set-up is shown in Figure 1 and the segmented detection plane is zoomed in Figure 2.

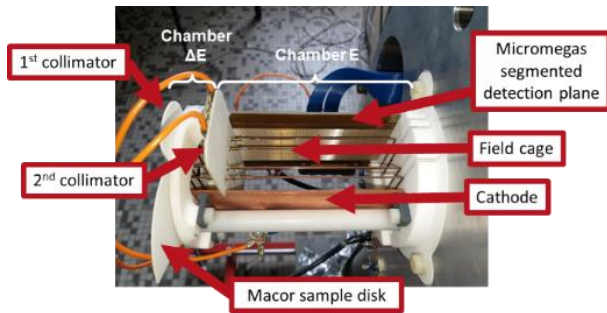


Fig. 1. Picture of the Gaseous Proton-Recoil Telescope

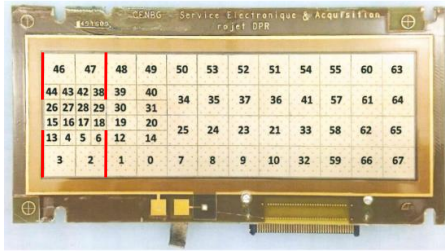


Fig. 2. Picture of the Micromegas detector plane. Red thick lines represent the places of both collimators

2.1 Detection system specific characteristics

As the aim of this detector is to detect proton recoil, it is of primary importance that as less protons as possible come from another source than the H rich sample. For this reason, the structures have been chosen to be of H-free materials: either of macor (collimators, sample disk, etc.), or metallic (cathode, field cage, etc.). For the same reason, the used gas is H-free: a mixture of N₂ and CO₂. The exact composition will be discussed in 3.4.

The pressure of the gas can be adapted to the neutron energy so the proton stops inside the detector. However, the H-rich foil thickness must also be adapted to the neutron energy so the loss of energy of the recoil proton is minor in the foil. For this reason, the sample disk has been designed to carry up to 8 H-rich foils. A motor allows to change the sample without opening the detector chamber. Its axis, not arrowed on Figure 1, is protected by an insulating plastic cylinder. The electric field, by the polarization voltages, is then adapted to the chosen pressure: as high as possible to maximize the amplification gain but low enough to avoid electrical breakdowns. Breakdown voltages have been

investigated as a function of the pressure and, to prevent micro-breakdowns, it has been chosen to work up to 20 V below the breakdown voltage.

To keep the proton recoil energy close to the neutron energy that created it, the proton scattering angle is limited thanks to the second collimator. The presence of this collimator allows a coincidence between the ΔE chamber and the E chamber, making this detector a telescope.

Finally, once the recoil proton is created, it will first pass through the first collimator, that clearly defines the sample active area, then through the second collimator to be detected in the E chamber. The segmented in 64 pads detection plane will collect each signal, allowing the reconstruction of the proton's track. Hence, only those activating pads in the ΔE and E chambers, passing through both collimators, are considered as correct. This allows to reject parasitic tracks.

2.2 Acquisition system

To get the proton tracks, the signals collected by the micromegas pads are treated by three successive cards: Zap, SAM and ZedBoard. The details of these cards are given in [14 (II.B) or 15]. Once treated by these cards, the signals are sent to the acquisition system composed of the Cobo software, developed by the CEA Saclay. Once saved, the events can be read by the CoboFrameViewer software, also developed by the CEA Saclay. As observed in the example of Figure 3, a frame is composed of 64 curves, each one corresponding to one pad response.

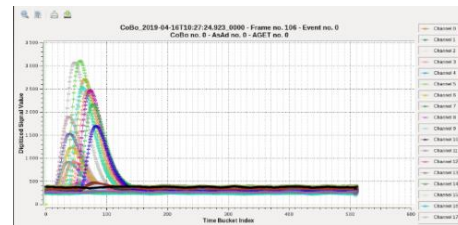


Fig. 3. Example of a frame saved by the Cobo software. Each curve corresponds to one pad.

3 Detection system characterization

Several tests have been carried out to develop the detector and check its reliability.

3.1 Sensitivity under irradiation

The aim of developing this detector is to be insensitive to gamma and electrons background, unlike silicon detectors. This has been checked with a neutron beam produced by the AIFIRA accelerator of the LP2I. When no H radiator was placed upstream the GPRT, only few tracks were observed by the acquisition system. Indeed, when the threshold, given in the software parameters, was adapted to protons, only very few cosmic rays' events could be detected, none coming from gamma nor electrons. This proves the low sensitivity of the GPRT

to background under irradiation. The results of this test have been published in [16].

3.2 Homogenization of the electric field

It has been checked that the electric field is stable and homogeneous under irradiation. This is possible thanks to the use of a field cage that can be adapted to the polarization voltages. Apart from minor edge effects, making the amplitude of the signals of the pads of the first and last columns dropping a bit, the field can be qualified as homogeneous. Under irradiation, the gain of the detector has proven to be constant. Indeed, issues of charge accumulation on insulating structures have been solved. The field is now stable under irradiation. The tests carried out and the results are presented in [16].

3.3 Tracks reconstruction and discrimination

As shown in Figure 3, each activated pad can be identified thanks to its curve. Hence, each track can be reconstructed with respect to the activated pads. An example of the track of a proton coming from the H-rich foil and passing through both collimators is shown in Figure 4.

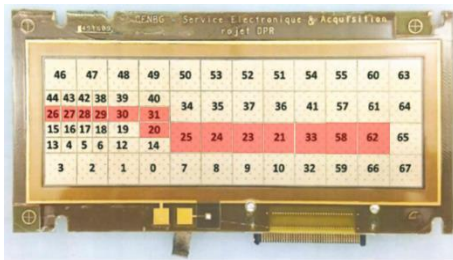


Fig. 4. Example of a track reconstructed based on the frame's curves.

Thanks to the track reconstruction, it is possible to discriminate the desired proton tracks, coming from the H-rich foil and created by a direct neutron, from any other particle. Indeed, a particle not coming from the H-rich foil may not pass through both collimators, as observed for example in Figure 5 (left) the track of a cosmic ray detected by the GPRT. Moreover, the track of a recoil proton from the H-rich foil but created by a scattered neutron will not have the same length in the GPRT, as the neutron energy will be lower than that of a direct neutron, as observed in Figure 5 (right).



Fig. 5. Example of a track reconstructed with respect to the frame's curves for a particle not coming from the H-rich foil (left) or coming from the H rich foil but from a scattered neutron (right).

Once the track of a wanted particle has been selected, it is possible to reconstruct the third dimension thanks to the electron drift time. Therefore, the reconstruction of

the track in three dimensions makes the GPRT a Time Projection Chamber (TPC). However, to have access to an accurate third dimension, the chosen gas inside the chamber must be slow so the electrons drift slowly to the anode. Indeed, one can consider the particle passing through the GPRT instantaneously, given the speed of the particle, and thus ionizing the gas everywhere at the same moment. With this condition, the electrons getting first to the anode are the one created the closest from this electrode, allowing a three dimensions track reconstruction as schemed in Figure 6.

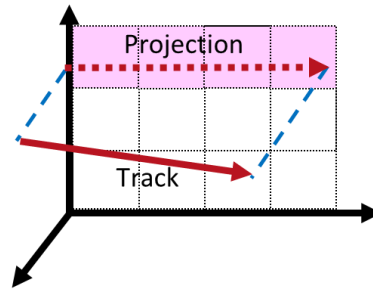


Fig. 6. Reconstruction of the third dimension thanks to the electron drift velocity

3.4 Choice of the gas

The gas needs to have good electric properties to allow the micromegas polarization without breakdowns and to enable an effective electrons multiplication. The chosen H-free gas is a mix gas composed of 70% of N_2 and 30% of CO_2 . First tests were performed with CF_4 . However, this gas is too fast inducing a poor time resolution which does not give access to the third dimension. Hence, the N_2-CO_2 mixture has been chosen for its low electrons drift velocity and good insulation properties. However, tests are currently carried out to find the optimal N_2/CO_2 proportions. Indeed, a higher ratio of CO_2 increases the gain (signal-to-background ratio increased) but a too high ratio of CO_2 creates breakdown problems due to a carbon deposit on the GPRT's elements. Investigations are still ongoing.

4 Tests with a proton micro-beam

4.1 Set up description

After the main characterizations and checks of the GPRT, the quantitative properties have been studied thanks to a proton micro-beam delivered by the AIFIRA facility. The rate of recoil protons during a cross section measurements would be around 1 proton/s. We thus need few protons/s entering the GPRT for our tests. To get such a beam, the initial beam was defocused and passed first through a micro collimator with a diameter of $20 \mu m$ standing at the entrance of a dedicated chamber (see Figure 7). An aluminum mylar window was used to separate the vacuum of the accelerator from the gas filled chamber. As both the first collimator and the window scatter protons, a second collimator of 2 cm upstream the detector was used. Downstream the GPRT, a silicon detector was used as reference. Finally, a set-

up inside the chamber allows to move the GPRT on two directions so the beam can be sent closer or further from the anode or on the side.

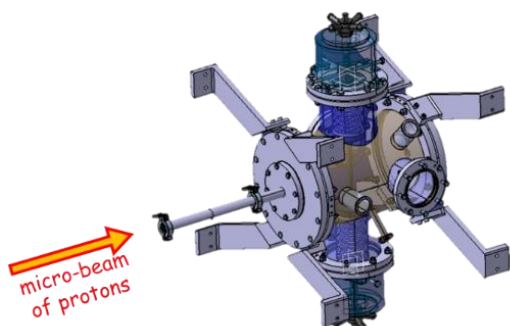


Fig. 7. Scheme of the designed chamber designed for this experiment.

4.2 Intrinsic efficiency

All the details of the intrinsic efficiency measurements can be found in [14, 15]. The intrinsic efficiency has first been studied with an alpha source delivering 4.5 alphas/s inside the GPRT. The efficiency was thus $(99.2 \pm 3.7^{\text{sys}} \pm 1.1^{\text{stat}})$ %, compatible with an intrinsic efficiency of 100%. This result has been checked with the proton micro-beam and confirmed for a rate of less than 3 protons/s. However, this efficiency decreases when the rate increases, down to 7% for 366 protons/s with a 50% efficiency for 38 protons/s. This problem has then been checked with an electronic bench test and it has been confirmed that it comes from the software or the hardware of the acquisition system. This issue is under investigation.

4.3 Energy and spatial resolution

The detection plane has quite large pads (0.5×0.5 cm² for the small ones) but it is still relevant to study the spatial resolution because the proton energy will be inferred via its range. It has been observed that the signal switched from one pad to its neighbor as the beam is shifted by 0.5 mm to the side. This effect is also observed when the primary electrons drift for 2 cm.

The energy resolution has also been studied thanks to the proton micro-beam. No quantitative results have been obtained but the energy resolution seems good enough for the requirements since the proton energy will not be reconstructed with the detected energy on each pad.

5 Conclusion

The GPRT is an almost-functional prototype that will be used to design the operational detector to measure neutron fluxes for fission cross section measurements. Its aim is to detect recoil protons for incident neutrons energy between 200 keV and 2.5 MeV.

As the GPRT allows the track reconstruction in three dimensions, this detector is a Time Projection Chamber.

The low sensitivity to gamma and electron background has been checked and validated under

irradiation. Thanks to a field cage that can be adjusted, the electric field is uniform and stable under irradiation. Some minor edge effects are still present but they only impact the first and last columns of pads. The energy and spatial resolutions have been investigated and present no constraint for our use. The intrinsic efficiency has been studied and is 100% for low protons rates and decreases when the rate increases. An investigation is carried out to improve the acquisition system performances.

Finally, once the intrinsic efficiency issue is solved, a new GPRT will be designed with (i) a more robust behavior with respect to breakdowns issues since they prevent a good reliability of the GPRT, (ii) a better design geometry to reduce the uncertainties of the geometric efficiency and (iii) the number of pads may be increased to get a better track reconstruction.

Acknowledgements: The authors would like to thank the AIFIRA team work, who helped for all the experiments, and the LP2I's electronic service, who is in help with all the acquisition's issues. This project has also received funding from the Euratom research and training program 2014–2018 under Grant No. 847552 (SANDA).

References

1. A.D. Carlson et al., *Evaluation of the neutron Data Standards*, « Nuclear Data Sheet », 2018
2. P. Marini, *et al.*, Nuc. Inst. Meas. in phys. A **841** 56-64 (2016)
3. P. Marini, *et al.*, Phys. Rev. C **96**, 054604 (2017)
4. S.J.Bame Jr, *et al.*, Rev. of Sci. Inst. **28**, 997 (1957)
5. T. Ryves, Nuc. Inst. and Met. in phy. **135**, 455 (1976)
6. R. Beyer, *et al.*, Nuc. Inst. and Met. in phy. A **575**, 449 (2007)
7. M.W. Wu, *et al.*, Nuc. Inst. and Met. in phy. A **422**, 79 (1999)
8. B. Daub, *et al.*, Nuc. Inst. and Met. in phy. A **701**, 171 (2013)
9. M. Kovash, *et al.*, *Detecting sub-MeV neutrons in solid plastic scintillator with gamma-ray discrimination*, in proceedings of the conference ANIMMA 2011, 6-9 Jun 2011, Ghent, Belgium (2011)
10. D. Schmidt, *et al.*, Nuc. Inst. and Met. in phy. A **476**, 186 (2002)
11. T.H.R. Skyrme, *et al.*, Rev. of Sci. Inst. **23**, 204 (1952)
12. E.F. Bennett, Rev. of Sci. Inst. **33**, 1153 (1962)
13. E.F. Bennett, T.J. Yule, Rad. Res. Soc. **50**, 219, 1972
14. C. Chatel, L. Mathieu et al., Eur. Phys. J. Web of Conferences **253**, 11013 (2021)
15. C. Chatel, PhD (2021)

<http://www.theses.fr/2021AIXM0416>

P. Marini, *et al.*, Eur. Phys. J. Web of Conferences **211**, 03010 (2018)